This is a repository copy of *Examination of Combustion-Generated Smoke Particles from Biomass at Source: Relation to Atmospheric Light Absorption*.

White Rose Research Online URL for this paper:
http://eprints.whiterose.ac.uk/141098/

Version: Accepted Version

Examination of Combustion-Generated Smoke Particles from Biomass at Source: Relation to Atmospheric Light Absorption

J.M. Jones[a], E.J.S. Mitchell[a], A. Williams[a], E. K. Barimah[a], G. Jose[a], N. Hondow[a], K.D. Bartle[a] and A.R. Lea-Langton[b,*]

[a] School of Chemical and Process Engineering. Leeds University, Leeds LS2 9JT, UK.
[b] Tyndall Centre for Climate Change Research, School of Mechanical, Aerospace and Civil Engineering, Manchester University, Manchester M13 9PL, UK.

*Corresponding author: e-mail: amanda.lea-langton@manchester.ac.uk

Abstract

The formation of carbonaceous aerosols from biomass combustion are associated with a high degree of uncertainty in global climate models. In this work, soot samples were generated from the combustion of pine wood, wheat straw and barley straw in a fixed bed stove; as well as from the combustion of biomass pyrolysis model compounds. Samples were collected on filters, which were used for the determination of Absorption Angstrom Exponent (AAE). In addition, the content and composition of elemental carbon (EC) and organic carbon (OC) were determined, and the interrelationships between these and the AAE were examined. It was found that the spectroscopic signature of samples with high 'brown carbon' emissions was comparable to that of many PAH and polyphenols, with AAE ranging from 1.0-1.2 for model compounds to 0.5-5.7 for biomass. In addition to the filter samples, particles were collected directly onto microscopy grids and analysed by transmission electron microscopy – electron energy loss spectroscopy (TEM-EELS) in order to determine structural characteristics. This was used to examine the impact of combustion conditions and flue gas dilution on particle structure. Smouldering phase and diluted particles were found to be less graphitic and twice as oxygenated as undiluted flaming phase particles. The results are interpreted to better understand the impact of combustion processes on soot formation from biomass combustion.

1. Introduction

The emission of smoke from the combustion of biomass in domestic stoves results in significant environmental problems which are dependent on the fuel type and the mode of combustion. Whilst the impact of greenhouse gas emissions from biomass combustion is relatively well understood, the role of aerosols remains highly uncertain in climate models due to limited data on particle optical properties. The major components of biomass carbonaceous aerosols are black carbon (BC) and organic carbons (OC). The former is a strong absorber of visible light and the latter may both absorb and scatter light across multiple wavelengths (Andreae and Gelencser, 2006; Bond and Bergstrom 2006). Polycyclic aromatic hydrocarbons (PAH) may be condensed onto the soot particles or be present as organic aerosols (OA), or in the vapour phase; tar balls are intermediate between soot and large PAH molecules (Bond et al., 2013., Lack et al., 2014). It has been proposed that BC is the second most important contributor to positive radiative forcing after that from carbon dioxide (Bond et al., 2013) whilst both BC and OC have a significant health impact (Orasche et al., 2013; Samburova et al., 2016). The way in which these are produced in the combustion system plays a major role although chemical reactions in the atmosphere play an important secondary role. This paper is only concerned with the role of the combustion processes and is an extension of work previously published by us (Atiku et al., 2016). The experimental measurement of the emission of BC and OC from a combustion process is undertaken either collecting a portion of the exhaust gases directly onto a filter paper or by using a diluted sample from a dilution tunnel.

Soot formed by the incomplete combustion of fossil or bio-fuels consists of chains of agglomerated carbonaceous spherules of elemental carbon (EC) with condensed organic compounds (OC). OC is also known as the volatile fraction or solvent extractable fraction. But in certain cases condensed partially decomposed cellulose products (such as levoglucosan) and lignin components (such as polyphenols) which can form organic aerosols (OA) may be produced (Atiku et al., 2016). The nature of the soot particle emitted depends on the nature of the fuel being burned, the conditions under which it is formed and the post-flame conditions (Orasche et al., 2013; Fachinger et al., 2017).

Fixed bed combustion of biomass undergoes three phases of combustion, initial ignition and flaming combustion stage mainly of the pyrolysed volatiles, and then via a transitional stage through to a smouldering phase. Once the first cycle is complete more fuel

2

may be added via refueling (often termed reloading). The flaming stage produces BC and associated soot-forming PAH precursors, the transitional and smouldering phases produces largely CO together with some BC and brown carbon (BrC). Brown carbon is a tar-like cellulose decomposition product resulting from the pyrolysis of incompletely combusted biomass material trapped within the core of burning biomass (Atiku et al., 2016).

Current atmospheric radiative models include contributions from both black carbon and organic carbon. BC is the dominant absorber of visible light although the term BC is subject to various interpretations (Lu et al., 2015; Lack et al., 2014). In these models OC was treated as purely scattering but it can absorb at shorter visible and UV wavelengths due to the presence of brown carbon (BrC) (Samburova et al., 2016). Atmospheric radiation models use the parameters single scattering albedo (SSA) and Absorption Angstrom Exponent (AAE) and these contain information on aerosol absorption (Andrea and Gelencser, 2006; Pokhrel et al., 2016). They are usually obtained by making measurements in the atmosphere using filter paper sampling or optical attenuation measurements. It has been suggested that SSA and AAE can be parameterized based on the modified combustion efficiency (MCE), the ratio of $[CO_2]/[CO$ and $CO_2]$ which is effectively a measure of incomplete combustion. However, evidence has been provided (Pokhrel et al., 2016) that the ratio EC/OC provides a better correlation.

A number of methods have been devised to measure BC, EC, OC and EC/TC (where TC = total carbon = EC + OC) or the equivalent BC/OC) from samples collected on filter papers. These can be analysed by using *in situ* optical methods using one or more wavelengths. Alternatively, thermo-gravimetric methods can be used alone or coupled with analysis of the released organic compounds, or by solvent extraction.

In the present experiments samples are taken directly from the flue gases from the combustion of pine wood, barley straw in a single burn (batch) stove and collected on a filter paper in a sampling system at a known collection temperature. Some samples were obtained from diluted flue gases using a dilution tunnel. Two model fuels, furfural and eugenol, which are typical biomass decomposition products were burned using a wick burner and in this case samples of soot were collected directly on to electron microscope grids.

Experimental Methods

The major source of the samples was a fixed bed stove (Waterford Stanley Oisin) rated as having a maximum thermal output of 5.7 kW and has previously been described (Atiku et al., 2016) and the main features are shown in Figure 1. The stove was mounted on an electronic balance to give the mass rate of burn. The fuels used were pine wood, barley straw and wheat with moisture contents of 7, 7, and 6 wt%s respectively. Total particulate matter (PM) in the flue gases was determined using a gravimetric method which required sampled gas passed through a preconditioned Munktell 360 Microquartz filter paper, with a second one used as a backing filter paper. The gas was taken via a heated line at 125°C and passed through the filter papers which were mounted in a heated block at 70°C. Three repeat measurements were taken during the flaming phase and during the smouldering phase for each fuel and the average taken. Some measurements were made using a dilution tunnel. All filter papers were stored in a desiccator for 24 h prior to measurement.
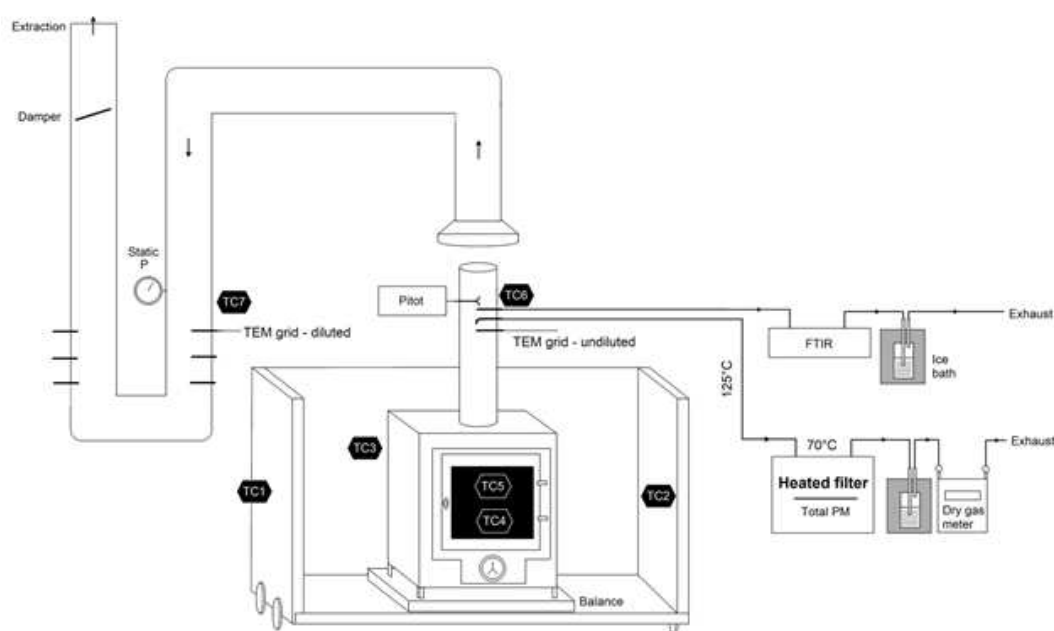
Figure 1. Combustion system and sampling arrangement for pine and straw fuels. Thermocouple measurement points are shown by TC#. Controlled temperatures of the heated sampling line and filter are indicated.

Secondly samples were obtained from a wick burner using model wood pyrolysis products, namely, furfural and anisole and also soot from n-decane. The wick burner is not a well controlled combustor but is the only way of burning high boiling point liquids and was

operated under carefully controlled combustion conditions previously described (Atiku et al., 2017). The soot samples were collected by a hood 20cm directly above the flame and sampled onto a filter paper as described above.

The Absorption Angstrom Exponents (AAE) of the filter papers were determined using a Perkin Elmer Lambda 950 UV-Vis-NIR Spectrophotometer over the range of 400-1200nm. The Absorption Angstrom Exponent is defined as:

$$b_{abs} = a \, \lambda^{-AAE} \qquad (1)$$

where b_{abs} is the absorption coefficient and the constant, a, is independent of wavelength. For small spherical soot particles AAE equals 1. The constant a is dependent on the thickness of the absorbing sample.

Thermogravimetric analysis (TGA) was used to measure the OC, EC and ash fractions for the pine samples as previously described (Atiku at al., 2016), and the thermo-optical method was used by Sunset Laboratories Inc. to determine EC/TC for the straw samples. The total carbon (TC) is the sum of the EC and the OC. Py-GC-MS was used in conjunction with sequential temperature pyrolysis for detailed analysis of the OC. The chromatograms were assigned on the basis of the NIST Mass Spectral Library Database, from previous literature and by known retention times. Soot sampling was undertaken directly onto the TEM grids, by impaction. The holey-carbon film grids were inserted into the flue for a measured time between 1-3 minutes depending on sample location and loading. The soot samples we examined by a FEI Titan[3] Themis transmission electron microscope (TEM) operating at 80kV and fitted with a Gatan One-View CCD and Quantum ER electron energy loss spectrometer. Care was taken such that electron energy loss spectroscopy (EELS) was conducted at the sample orientation independent angle (Daniels et al., 2003), and on a region of sample entirely over a hole in the carbon film filling the area of the selected area aperture to eliminate any carbon signal from the TEM support grid. EELS measurements were carried out with a collection angle of 6 mrads, a convergence of 1 mrad and a dispersion of 0.5 eV/channel. A power law background fit was applied before C K-edge (285 eV) and first order log polynomial fit before O K-edge (532 eV), with a 60 eV integration window and HS cross-sections. There are a limited number of TEM-EELS datasets exploring soot morphology and composition from stoves using dilution tunnels. Only with the latest techniques has it been possible to estimate the carbon, oxygen, nitrogen and sp2 contents of

individual soot particles collected on TEM grids, removing the need for invasive filter extraction techniques. The percentage of sp2 orbital hybridisation in particle atomic structure (%sp2) is a useful indicator of graphitic and amorphous structures in carbonaceous samples, whereby higher values indicate more graphitization as is expected of highly ordered soot particles.

2. Experimental Results

3.1 Experimental Results using Filter Paper Samples

Samples of soot were collected on filter papers from the combustion of pine and straw under flaming and smouldering phases of combustion, and from the model biomass pyrolysis compounds, anisole and furfural, burning on a wick burner. These samples are of soot particles and the primary organic matter (POM) and have not been subject to ageing which would substantially increase the mass of the POM (Corbin et al., 2015).

Figure 2 shows typical examples of the attenuation due to absorption of anisole and furfural soot, samples of pine wood, barley and wheat straw soot under different conditions in the wavelength range of 400 to 2000nm. Using OriginLab software, the absorption spectrum was fitted with exponential function described in Eq. 1 to determine the AAE value. This procedure was used to determine AAE values for the samples shown in Figure 2, pine, and two straws, wheat and barley straw. Thicker samples show band spectra for PAH and O-PAH compounds which have been observed in biomass combustion (Massabo et al., 2015).
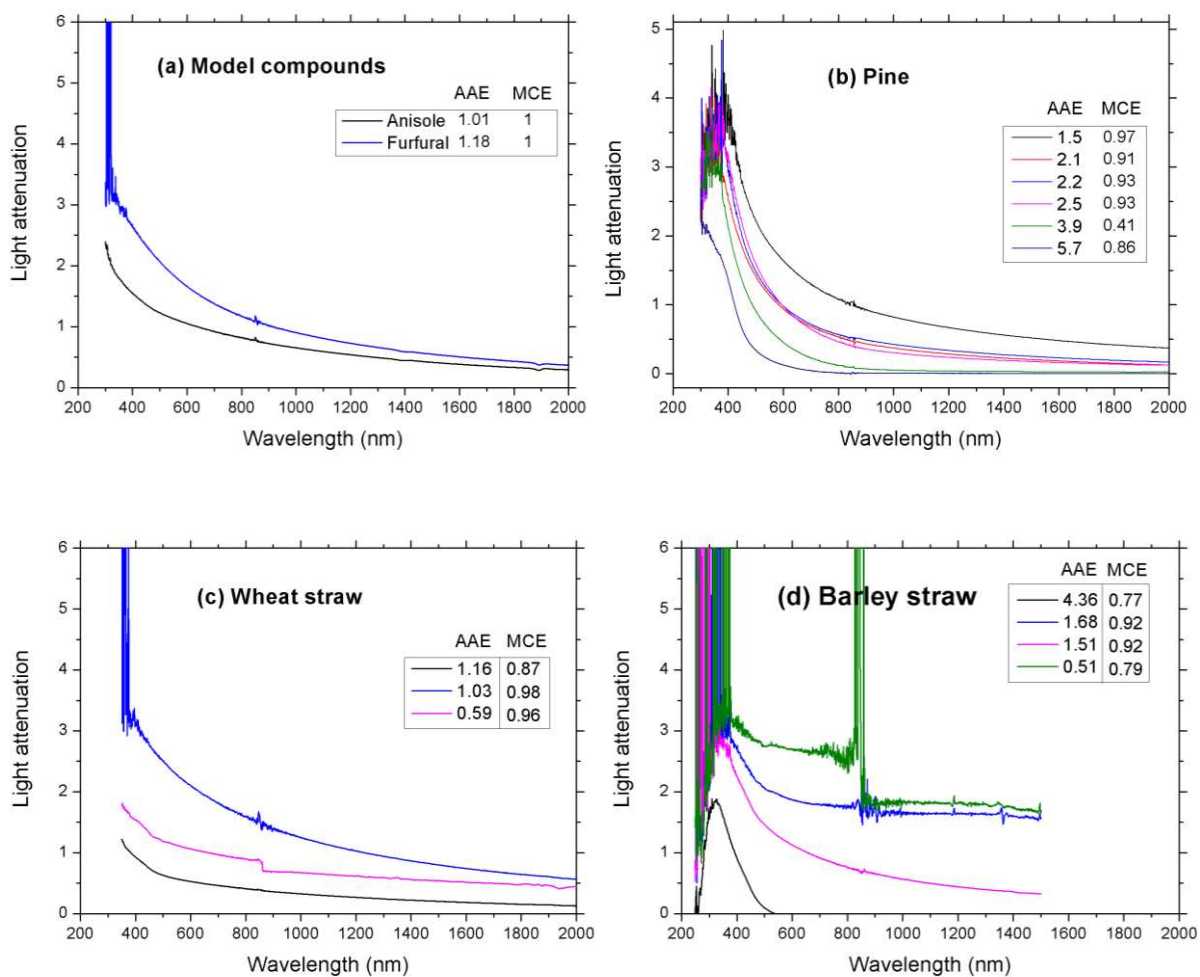
Figure 2. Spectra for individual filter samples for (a) model compounds, (b) pine, (c) wheat straw, (d) barley straw. Each filter sample was taken at a different stage in the combustion cycle, as denoted by the different values of MCE.

In all the cases shown in Figure 2 the shapes of the attenuation/absorption spectrum vary with AAE. An extensive set of relevant PAH spectra has been given by Izawa et al., (2014) and it

is apparent that the PAH species alone could not explain the shapes of these curves. In the 400 – 800 nm region it is probably partially caused by polyphenols.

The values of the Absorption Angstrom Exponents are summarised in Table 1 together with the color of the filter deposit and values obtained for EC/OC. The modified combustion efficiency, MCE, defined by the ratio of $[CO_2]/[CO$ and $CO_2]$ are also given. Most of the results were obtained using thermal analysis methods but those for straw were obtained using the optical method. Fig.2 shows examples of filters taken across the full burn cycle for single experiments for the fuels. These examples are not necessarily the same as the ones in Table 1, although it is the case for most fuels but not for pine. The Fig.2 pine curve is provided to show clearly the transition from low AAE to high AAE. Correction factors can be applied to filter-based measurements of particle optical properties for filter loading and scattering effects which may skew the results. The corrected black carbon concentration can be related to the uncorrected BC concentration, BCi, by the formula

$$BC_{corrected} = (1 + k \text{ ATN}) BCi, \qquad (2)$$

where k is the loading correction factor and ATN the light attenuation at a given wavelength (Virkkula et al., 2007). The factor k is dependent on the sampling system and aerosol type, as well as the filter substrate and the wavelength used in measurements. Here the samples were taken on quartz fibre filters and under these conditions it was concluded that for these samples a correction factor of unity should be applied (Davy et al., 2017; Segura et al., 2014)

Table 1 Absorption Angstrom Exponent (AAE) and properties of the samples

Fuel	Absorption Angstrom Exponent	Colour of the soot sample collected	Modified combustion efficiency (MCE)	EC/TC
Anisole	1.01	fluffy black	1	0.98
Furfural	1.18	black	1	0.98
Pine wood, flaming	0.99	black	0.93	0.5
Pine wood, transition	1.91	brown	0.65	0.3
Pine wood, smouldering	3.33	yellowish	0.63	0.1
Barley straw, flaming	0.51	black with blue-grey tinge	0.79	0.78
Wheat straw, flaming	1.16	grey-brown	0.87	0.26
	Average AAE			
Fuel	Flaming (SD)		Smouldering (SD)	
Pyrolysis Model compounds	1.10 (0.09)		-	
Barley straw	1.09 (0.58)		2.93 (1.43)	
Wheat Straw	0.81 (0.22)		1.16 (0)	
Pine wood	1.24 (0.25)		3.09 (1.26)	

It is seen the value for AAE for anisole, an aromatic compound which gives a highly carbonaceous soot, is 1.01. Furfural which produces a more oxygenated OC had a slightly higher value (1.18). The values for flaming combustion for wood are close to unity, but for smouldering combustion the values are higher, again consistent with the formation of brown carbon (Massabo et al., 2015). The colouring matter of biomass originates in the UV/visible spectra of polyphenols which absorb between 350 and 550 nm due to the presence of

flavonoids, generally containing glycosidic structures; these are present as a result of thermal decomposition of cellulosic materials (Anouar et al., 2012).

3.2 Results from Py-GC-MS Experiments

The samples collected on the filters consists of both the soot together with some surface PAH as well as condensed high molecular weight PAH which would be emitted in the form of organic aerosols (OA). Measurements were made of the PAH emissions in the flue gases under flaming and smouldering conditions. In the former a range of species were observed, the most abundant ones being: phenanthrene, fluoranthene and pyrene. Other PAH observed included, naphthalene, acenaphthylene, anthracene, benz[*a*]anthracene, chrysene, benzo[*b*]fluoranthene, benzo[*k*]fluoranthene and benzo[*a*]pyrene. Of these, phenanthrene and pyrene are protographenes, and the fluoranthenes are protofullerenes. Smouldering combustion emissions were different since the PAH levels were lower and especially the larger PAH species were in a much smaller concentration.

From earlier studies (Ross et al., 2002) using a wood stove it was found that the products included: total PAH: 14000 µg/MJ fuel burned; alkylated PAH: 7600 µg/MJ fuel burned, and phenols: 13000 µg/MJ fuel burned. Similar oxygenated species to those shown in Table 2, were found to be produced in an open wood fire (Ross et al., 2007).

Table 2. Major species identified in the soot organic fractions at different pyrolysis temperatures for pine wood and furfural: a model oxygenated biomass pyrolysis product

Pyrolysis T	**Wood Stove: pine wood**	**Furfural flame**
400°C	methoxyphenols methyl-furans, levoglucosan, sugars	alkanes, oxygenated species: carboxylic acids and esters
500°C	phenols, methyl and methoxy phenols, furans, anisole	traces of methoxyphenols
600°C	traces of aldehydes, phenols	no significant peaks-suggesting no large molecules

3.3 Studies of Soot Samples Extracted from the Flame Gases from pine Combustion

TEM photographs obtained from the combustion of pine in the stove are shown in Figures 3-5. These show that soot samples produced for both flaming and smouldering combustion are not significantly different in any respect. Particle size studies (e.g. Ting et al., 2018) have shown that are 20 nm and 100 nm particles present in a bi-modal distribution in biomass combustion. When a dilution tunnel is used with a dilution factor of 12 there is increased branching and agglomeration of particles in the dilution tunnel compared to freshly emitted particles. This is shown in Figure 5 particularly by the 500 nm scale images. Clearly the degree of agglomeration is not just a feature of the combustion process but also by dilution of the flue gases (Singh et al., 2014), a step that is always present in real combustion systems.
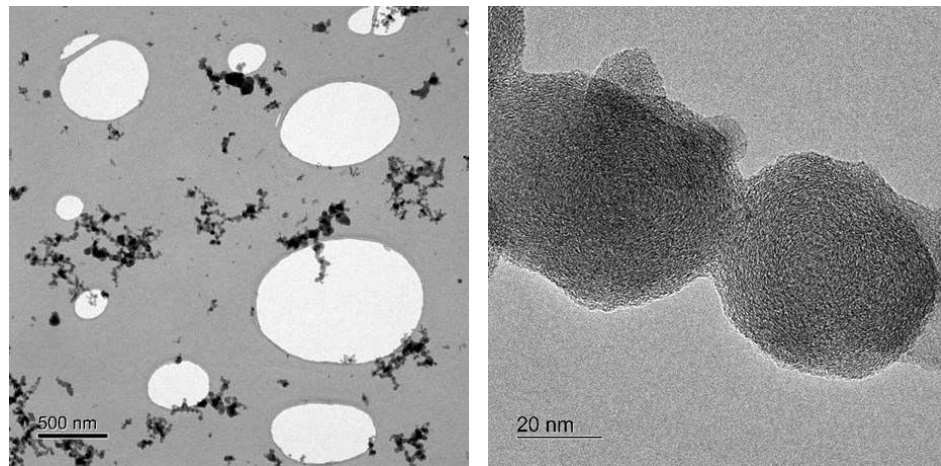

Figure 3. TEM image of pine soot taken from the flue gas during the flaming phase
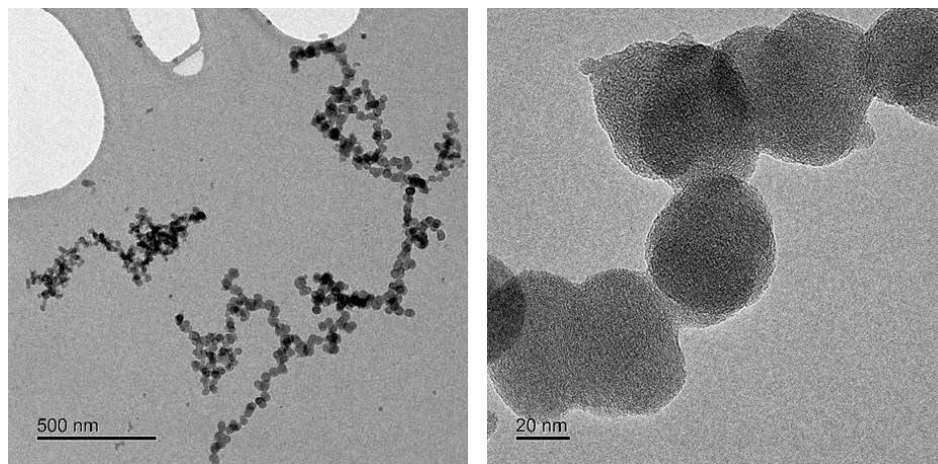

Figure 4. TEM image of pine soot taken from the flue gas during the smouldering phase.
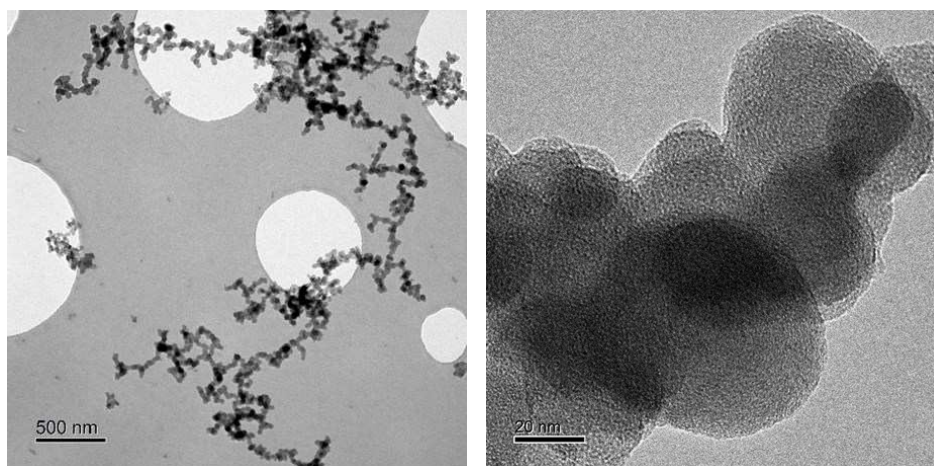
11

Figure 5. TEM image of pine soot taken from the dilution during flaming phase

Electron Energy Loss Spectroscopy (EELS) analysis of the structures of the soot samples was made and the results for sp2 and C:O are given in Table 3. The degree of sp2 in relation to sp3 shows the extent of graphitisation. The dilution tunnel has a marked effect on the sizes of the soot chains, these samples also show increased oxygenation and the sp2 content is slightly lower for dilution tunnel samples. It is seen that a distinct nitrogen peak was found for the samples, increasing for the smouldering case

Table 3; Summary of the EELS results, elements in atomic %

Sample	%SP2	C (%)	N (%)	O (%)
Dilution tunnel	60.5 (n=10)	88.0 (n=4)	1.6 (n=4)	10.4 (n=4)
Flaming phase	66.5 (n=10)	93.3 (n=8)	1.3 (n=8)	5.4 (n=8)
Smouldering phase	64.3 (n=8)	92.4 (n=7)	1.7 (n=7)	5.9 (n=7)

n = number of spectra used to generate each average value in the table

The presence of both O and N in soot and PAH is known (Ross et al., 2007; Mohr et al., 2013), however these species are not included in current soot forming models and it is usually assumed that they are formed after the main flame reactions are completed. Increasing the degree of fuel oxygenation leads to an increasing degree of amorphous nanostructure (Vander

Wal and Mueller, 2006). Newly formed soot and PAH have abundant free electrons available that enables them to react with both O_2 and NO present in the hot combustion gases. The increase in –O- in the soot samples in the dilution tunnel (Table 3) are consistent with that effect. Nitrated phenols are a significant constituent of biomass burning secondary organic aerosol and contribute to the light absorbing fraction of organic carbon (Mohr et al., 2013).

3. Discussion

The general steps of soot formation from biomass are largely understood but in the most part are based on studies of the combustion of hydrocarbon fuels in the gas phase. This general mechanism is shown in outline in Figure 6 where the low molecular weight PAH initially formed arises from the primary radical products from cellulose decomposition via the HACA route (Fitzpatrick et al., 2008) or react through the CPDyl route (Atiku el al., 2017). Other devolatilisation products of the biomass may also be present, for example, sugars and resinous constituents of coniferous wood. Biomass soot formation includes a major route from lignin decomposition which forms large amounts of oxygenated compounds such as methoxyphenols. It should be noted that the formation of Brown Carbon would form an additional route which involves incomplete combustion because of lack of oxygen or because the fuel particle is large.
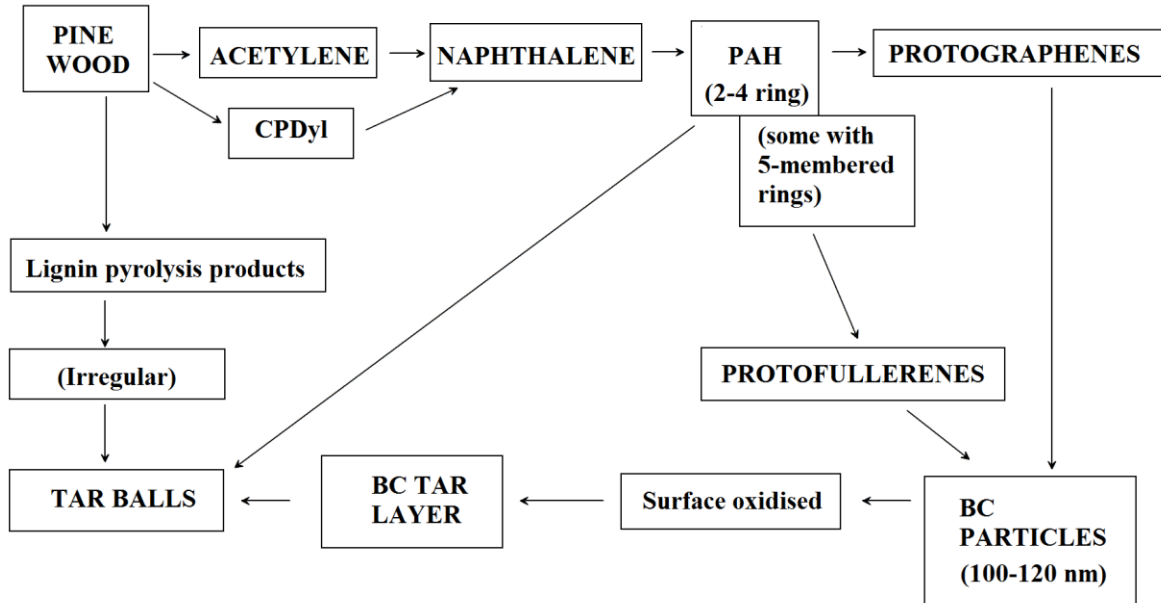
Figure 6 Outline mechanism of the formation of soot and tar balls.

The data obtained for the Absorption Angstrom Exponent (AAE) in Table 1 may be related to the modified combustion efficiency (MCE) This parameter base on the CO concentration will be indicative of the amount of other unburned organic compounds such as CH_4 and CH_2O emitted (Ndiema et al., 1998). Figure 7 shows a plot of AAE against MCE for pine and oak wood, wheat and barley straw, and also anisole and furfural. In such a plot the 'highly carbonaceous' soot from anisole should tend to be in the right hand bottom corner of Figure 7 tending towards the values of AAE =1 and MCE = 1. Whilst all the points suggest a trend between AAE and MCE a trend line is not given because of the large scatter.
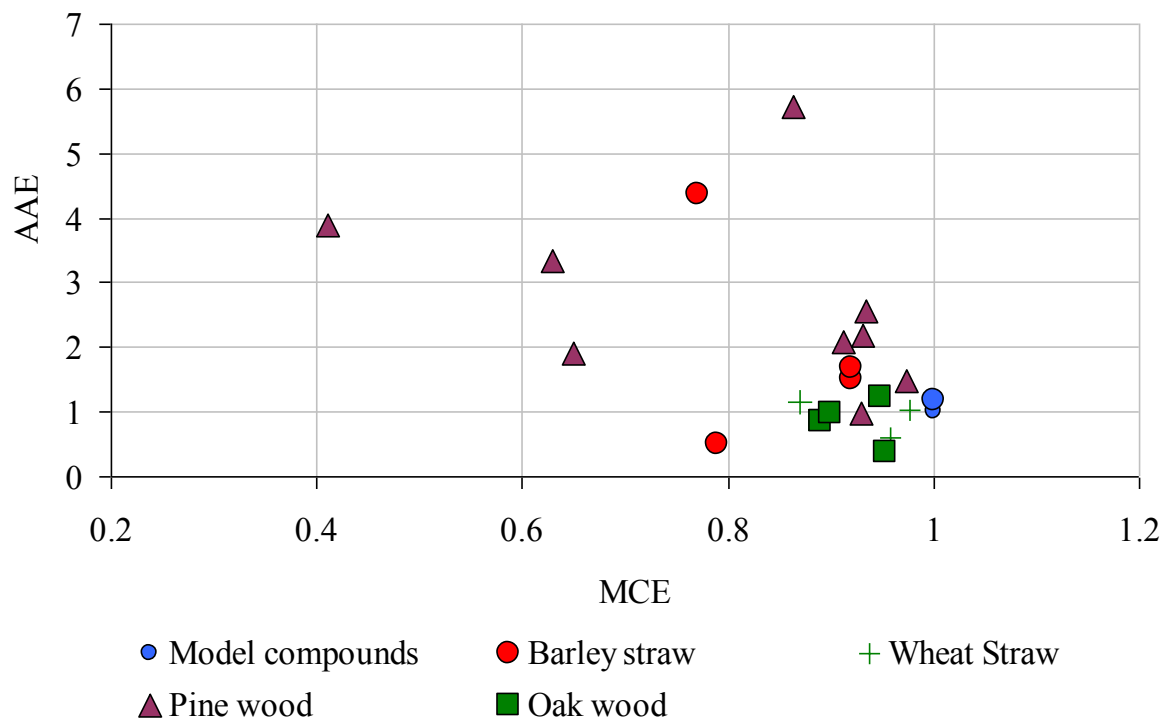
Figure 6. Variation of Absorption Angstrom Exponent (AAE) with Modified Combustion Efficiency MCE).

From the limited evidence here, it seems that AAE is more dependent on MCE than fuel type. This arises because as combustion becomes less complete as shown by a decreasing value of MCE not only does CO increase but also associated species of incomplete combustion such as CH_4, CH_2O and other oxygenated species increase. Apart from a slight blue-grey tinge in a small number of straw soot samples, the differences between woods and the straws is small, yet the difference between 'pure' carbons from the model fuels is significant. Pokrel et al. (2016) have shown parameterizations of AAE based on the elemental carbon (EC) to organic carbon (OC) mass ratio are quantitatively superior to parameterizations based on MCE. However, the way that AAE is determined is dependent on the temperature at which the filter sample is measured. This is because the combustion conditions will determine the profile of combustion species produced, so that CO is the major product, followed by CH_4, the aliphatic hydrocarbons, PAH and oxygenated species in a sequence determined by their thermodynamic stability (Jones et al., 2017). The filter temperature determines the range of species seen for the AAE measurement. Thus, there is a significant difference between results obtained directly from a stove, as in this case, in comparison with those observed after

dilution or by sampling in the atmosphere. Brown Carbon presents a special case since it is an incompletely reacted species and not in chemical equilibrium with the other species.

Brown Carbon (BrC) consists largely of primary aerosols of high molecular weights and will all be collected by condensation onto filter papers, the degree of collection is dependent on the sampling temperature (70ºC in this study). It is likely that BrC consists of two classes of components, largely sugar-derived pyrolysis products arising from the incomplete combustion of cellulose and large PAH compounds including some polyphenols and nitro-polyphenols. The sugar derived products are formed from partially pyrolysed biomass in the centre of large biomass particles mainly during the smouldering phase-from which the partially reacted products can escape through cracks or large pores. The second group result from the reaction of some of the large stable PAH with nitric oxide or dioxide in the flame zone, although it can also be formed by reactions occurring in the atmosphere. Inferences as to the chemical nature of the BrC layer can be drawn from solid-state reflectance spectra of the surface (Izawa et al., 2014). A comparison of spectra with those of complex mixtures of aromatics such as coal tar pitch can give an indication of the chemical nature of BrC. Thus, coal tar pitch has been shown (Koolen et al., 2015) to be a mixture of individual compounds, largely PAH substituted with heteroatomic groups such as polyphenols, many multifunctional; the spectrum of the pitch is an intense unresolved absorption band with a maximum near 330 nm decreasing to zero at about 600 nm. These wavelengths suggest that the BrC absorptions can be attributed to structures differing from those in the BC spectra which consist of gently-declining absorptions extending into the IR beyond 1500 nm from BC particles.

The values of EC/TC also depend on the way in which they are determined, in particular whether they are measured by gravimetric, optical or aerosol time of flight mass spectrometer (ATOFMS) techniques. Previously we have used ATOFMS for measurements of the EC/TC ratio in smoke from both wood directly above the flame (Lea-Langton et al., 2015). For softwood (pine) these values were 0.61 during flaming combustion and 0.62 during smouldering combustion. These are similar to those obtained in other studies (Elsasser et al., 2013).

In the present work we report values of EC/TC for flaming and smouldering conditions (Table 1) obtained using filter paper sampling where there is a significant

difference between the values for flaming and smouldering conditions. Other studies, for example (Elsasser et al., 2013) also show that when using the filter sampling method there is a significant difference between 'good' combustion, that is, flaming combustion, and 'poor' combustion, that is, smouldering combustion, and cases where the large size of the fuel causes internal pyrolysis prior to combustion.

This contrasts with the ATOFMS methods and is clearly linked to the fact that the filter paper sampling method collects the entire sample, i.e. carbonaceous particles together with inherent PAH as well as independent OC, the amount depending on the filter temperature (Jones et al., 2017). The ATOFMS method measures only the inherent PAH and consequently there is a similarity between EC/TC for both flaming and smouldering since the soot forming reactions are the same in both cases, as indicated in Figure 6.

4. Conclusions

- Smoke samples have been taken directly from the flue gases of a domestic stove and from combustion of biomass model compounds. Analysis of these enabled optical property measurements to be made which suggested potential climate impact due to the brown carbon content.

- Comparison between dilution tunnel samples and the direct flue samples showed that there was a significant degree of oxidation occurring during the dilution process. However, the particulate nitrogen levels did not change after the combustion process. The EELS analysis also showed slightly less degree of graphitisation in the diluted samples.

- Brown Carbon is chemically and optically different to black carbon and the mechanism of formation is largely due to the low temperature pyrolysis in large particles of biomass. The observed colour of the filter papers gave an indication of the presence of oxygenated organic compounds and PAH.

- A weak relationship was observed between the AAE and MCE, with the pyrolysis model compounds giving an AAE of 1 for MCE of 1 (100% efficient combustion), whereas low MCE combustion (representing smouldering conditions) had a higher AAE, indicating a greater potential impact towards climate change.

List of abbreviations

AAE	Absorption Angstrom Exponent
ATN	Light attenuation
AToFMS	Aerosol time of flight mass spectrometer
BC	Black carbon
BrC	Brown carbon
C:O	Carbon to oxygen ratio
CPD	Cyclopentadienyl radical C5H5
DMS	Differential mobility spectrometer
EC	Elemental carbon
EELS	Electron energy loss spectroscopy
HACA	Hydrogen abstraction carbon addition
MCE	Modified combustion efficiency
OA	Organic aerosols
OC	Organic carbon
PM	Particulate matter
POM	Primary (particulate)organic matter
Py-GC/MS	Pyrolysis gas chromatography/mass spectrometry
sp2	Amount of sp2 orbital hybridisation in atomic structure
SSA	Single scattering albedo
TC	Total carbon (BC+OC) or (EC+OC)
TEM	Transmission electron microscope
TGA	Thermogravimetric analysis

Acknowledgements

References

Andreae, M.O., and A. Gelencser, A. 2006. Black carbon or brown carbon? The nature of light-absorbing carbonaceous aerosols, *Atmos. Chem. Phys*., **6,** 3131−3148.

Anouar, E.H., Gierschner, J., Duroux, J-L., Trouillas, P. (2012). UV/Visible spectra of natural polyphenols: A time-dependent density functional theory study, *Food Chemistry,* **131,** 79–89.

Atiku, F.A., Mitchell, E.J.S., Lea-Langton, A.R., Jones, J.M., Williams, A., and Bartle, J.D. 2016. The impact of fuel properties on the composition of soot produced by the combustion of residential solid fuels in a domestic stove, *Fuel Proc. Technol.,* **151,** 117–125.

Atiku, F.A., Lea-Langton, A.R., Bartle, K.D. Jones, J.M., Williams, A., Burns, I., and Humphries, G. 2017. Some aspects of the mechanism of formation of smoke from the combustion of wood, *Energy Fuels,* **31,** 1935−1944.

Bond, T.C., and Bergstrom, R.W., 2006. Light absorption by carbonaceous particles: an investigative review, *Aerosol Sci. Technol.,* **40,** 27-67.

Bond, T.C., Doherty, S.J., Fahey, D.W., Forster, P.M., Berntsen, T. et al., 2013. Bounding the role of black carbon in the climate system: A scientific assessment, *J. Geophys. Res.,* **118,** 5380−5552.

Corbin, J.C., Keller A., Lohmann, U., Burtscher, H., Sierau, B., and Mensah A.A., 2015. Organic emissions from a wood stove and a pellet stove before and after simulated atmospheric aging, *Aerosol Sci Technol.,* **49,** 1037-1050

Daniels, H., Brown, A., Scott, A., Nichells, T., Rand, B., and Brydson, R., 2003. Experimental and theoretical evidence for the magic angle in transmission electron energy loss spectroscopy. *Ultramicroscopy,* **96**, 523–534.

Davy, P.M., Tremper, A.H., Nicolosi, E.M.G., Quincey, P., and Fuller, G.W. 2017. Estimating particulate black carbon concentrations using two offline light absorption methods applied to four types of filter media. *Atmos. Environ.,* **152,** 24-33.

Elsasser, M., Busch, C., Orasche, J., Schon, C., Hartmann, H., Schnelle-Kreis, J., and Zimmermann, R. 2013. Dynamic changes of the aerosol composition and concentration during different burning phases of wood combustion. *Energy Fuels,* **27,** 4959-4968.

Fachinger, F., Drewnick, F., Giere, R., S. and Borrmann, S. 2017. How the user can influence particulate emissions from residential wood and pellet stoves: Emission factors for different fuels and burning conditions, *Atmos Environ.,* **158,** 216-226.

Fitzpatrick, E.M., Jones, J.M., Pourkashanian, M., Ross, A.B., Williams A. and Bartle, K.D., 2008. Mechanistic aspects of soot formation from the combustion of pine wood. *Energy Fuels,* **22,** 3771-3778.

Izawa, M.R.M., Applin, D.M. Norman, L. and Cloutis, E.A. 2014. Reflectance spectroscopy (350–2500 nm) of solid-state polycyclic aromatic hydrocarbons (PAHs). *Icarus,* **237,** 159-181.

Jones J.M., Ross A.B., Mitchell E.J.S. Lea-Langton A.R., Williams A., and Bartle. K.D., 2017. Organic carbon emissions from the co-firing of coal and wood in a fixed bed combustor. *Fuel,* **195,** 226-231.

Koolen, H.F., Swarthout, R.F., R.K. Nelson, H. Chen, L.C. Krajewski, C. Aeppli et al, 2015. Unprecedented Insights into the chemical complexity of coal tar from comprehensive two-dimensional gas chromatography mass spectrometry and direct infusion Fourier Transform ion cyclotron resonance mass spectrometry. *Energy Fuels,* **29,** 641-648.

Lack, D.A., Moosmüller,H., McMeeking, G.R., Chakrabarty, R.K., and Baumgardner, D. 2014. Characterizing elemental, equivalent black, and refractory black carbon aerosol particles: a review of techniques, their limitations and uncertainties. *Anal. Bioanal. Chem.,* **406,** 99-122.

Lea-Langton, A.R., Baeza-Romero, M.T., Boman, G.V., Brooks, B., Wilson, A.J.M., Atiku, F., Bartle, K.D., Jones, J.M., and Williams, A. 2015. A study of smoke formation from wood combustion. *Fuel Proc Technol.,* **137,** 327–332.

Lu, Z., Streets, D.G., Winijkul, E., Yan, E., Chen,Y., Bond, T.C., Feng, Y.,M.K. Dubey, M.K., et al., 2015. Light absorption properties and radiative effects of primary organic aerosol emissions. *Environ. Sci. Technol.,* **49,** 4868−4877.

Massabo, D. L., Caponi, L., Bernardoni, V., Bove, M.C., Brotto,. P., Calzolai, G., Cassola,F. et al., 2015. Multi-wavelength optical determination of black and brown carbon in atmospheric aerosols. *Atmos. Environ*., **108,** 1-12.

Mohr, C., Lopez-Hilfiker, F.D., Zotter, P., Prevot, A.S.H. Xu, L., Ng, N.L., Herndon, S. C., Williams, L. R., Franklin, J. P., et al., 2013. Contribution of nitrated phenols to wood burning brown carbon light absorption in Detling, United Kingdom during winter time. *Environ. Sci. Technol.,* **47,** 6316−6324.

Ndiema, C.K.W., Mpendazoe, F.M., and Williams, A. 1998. Emissions of pollutants from a biomass stove. *Energy Convers Manage.*, **39,** 1357-1367.

Orasche, J., Schnelle-Kreis, J., Schön, C., Hartmann, H., Ruppert, H., Arteaga-Salas, J.M. and Zimmermann, R. 2013. Comparison of emissions from wood combustion. Part 2: Impact of combustion conditions on emission factors and characteristics of particle-bound organic species and polycyclic aromatic hydrocarbon (PAH)-related toxicological potential. *Energy Fuels,* **27,** 1482−1491.

Pokhrel, R.P., Wagner, N.L., Langridge, J.M., Lack, D.A. Jayarathne, T., Stone, E.A., Stockwell, C.E., Yokelson, R.J., and Murphy, S.M. 2016.Parameterization of single-

scattering albedo (SSA) and Absorption Ångström Exponent (AAE) with EC/OC for aerosol emissions from biomass burning. *Atmos. Chem. Phys.,* **16,** 9549–9561.

Ross, A.B., Jones, J.M., Chaiklangmuang, S., Pourkashanian, M., Williams, A., Kubica, K., Andersson, J.T., Kerst, M., Danilhelka, P and Bartle, K.D. 2002. Measurements and prediction of the emission of pollutants from the combustion of coal and biomass in a fixed bed. *Fuel,* **81,** 571-582.

Ross, A.B., Fitzpatrick, E.M., Bates, J., Andrews, G.E., Jones, J.M., Phylaktou, H., and Williams, A. 2007. Emission of oxygenated species from the combustion of pine wood and its relation to soot formation, *Process Saf. Environ.*, **85(b5),** 430-440.

Segura, S., Estellés, V., Titos, G., Lyamani, H., Utrillas, M.P., Zotter, P., et al., 2014. Determination and analysis of in situ spectral aerosol optical properties by a multi-instrumental approach. *Atmos. Meas. Tech.,* **7,** 2373–2387.

Singh, S., Adams, P.J., Misquitta, A., Lee, K.J., Lipsky, E.M., and Robinson A.L. 2014. Computational analysis of particle nucleation in dilution tunnels effects of flow configuration and tunnel geometry. *Aerosol Sci. Tech.,* **48,** 638-648.

Samburova, V., Connolly, J., Gyawali, M., Yatavelli, R.L.N., Watts, A.C., Chakrabarty, R.K., Zielinska, B., Moosmüller, H. 2016. Polycyclic aromatic hydrocarbons in biomass-burning emissions and their contribution to light absorption and aerosol toxicity, *Sci. Total. Environ.* **568**, 391–401.

Ting, Y., Mitchell, E.J.S., Allan, J.D., Liu, D., Spracklen, D.V., Williams, A. Jones, J.M., Lea-Langton, A.R., McFiggans, G. and Coe, H. (2018). Mixing state of carbonaceous aerosols of primary emissions from "improved" African cookstoves, Environ. Sci. Technol. **52**, 10134–10143.

Vander Wal, R.L. and Mueller C.J. 2006. Initial investigation of effects of fuel oxygenation on nanostructure of soot from a direct-injection diesel engine. *Energy Fuels,* **20,** 2364-2369.

Virkkula, A., Mäkelä, T., Risto Hillamo, R., Yli-Tuomi T., Hirsikko A., Hämeri, K., and Koponen, I.K. 2007. A simple procedure for correcting loading effects of aethalometer data. J. *Air Waste Manage. Assoc.,* **57**, 1214 -1222.